MATERIALE PLASTICE
https://revmaterialeplastice.ro
https://doi.org/10.37358/Mat.Plast.1964

Insight into the Role of a Isophthalic Dihydrazide Derivative Containing Piperonylic Acid in Poly(L-lactide) Nucleation: Thermal Performances and Mechanical Properties

HAO HUANG[1], YAN-HUA ZHANG[1], LI-SHA ZHAO[1], GUANG-MING LUO[2], YAN-HUA CAI[1]*

[1]Chongqing Key Laboratory of Environmental Materials & Remediation Technologies, Chongqing University of Arts and Sciences, Chongqing-402160, P.R. China
[2]The Nanchuan District in Chongqing LongHua Vocational School, Chongqing- 408400, P.R. China

Abstract: *This work was aimed at synthesizing the N, N'-isophthalic bis(piperonylic acid) dihydrazide (PAID) to be as a new crystallization accelerator for poly(L-lactide) (PLLA), and a detailed investigations of the non-isothermal crystallization, melting behavior, thermal decomposition behavior and mechanical properties of PLLA nucleated by PAID were performed applying differential scanning calorimetry (DSC), thermogravimetric analysis (TGA) and electronic tensile tester. The melt-crystallization proved that the PAID could act as a heterogeneous nucleating agent to significantly promote the crystallization in cooling, even the crystallization was still able to be accelerated upon the fast cooling at 50 °C/min. The final melt temperature was another crucial factor for PLLA's melt crystallization, and when the final melt temperature was 170 °C, the onset crystallization temperature and melt-crystallization enthalpy was almost up to 150 °C and 56.8 J/g upon cooling of 1 °C/min, respectively. Furthermore, the chemical nucleation was proposed to be the nucleation mechanism of PAID for PLLA via the preliminary theoretical calculation. For the cold-crystallization, the addition of PAID exhibited an inhibition for the crystallization of PLLA, but the total crystallization process depended on the heating rate and PAID concentration. The single melting peak after cooling of 1 °C/min indicated that the crystallization had been thoroughly completed in cooling. Additionally, the single melting peak with different locations after full crystallization resulted from the different crystallization temperatures. A comparison in the onset decomposition temperature implied that the presence of PAID only slightly decreased the thermal stability of PLLA. The mechanical testing showed that, in contrast with the elongation at break, the existence of PAID enhanced the tensile strength of PLLA.*

Keywords: *poly(L-lactide), nucleating agent, crystallization, piperonylic acid, isophthalic dihydrazide*

1.Introduction

Poly(L-lactide) (PLLA), as a configuration of poly(lactic acid), can be obtained from renewable resources such as potato, corn, rice, etc. [1, 2], which dramatically reduces the usage of fossil resources and hazard of white pollution. Moreover, these typical features of PLLA itself including inherent biodegradability, excellent biocompatibility, nontoxic, relatively low-cost production [3, 4] leads to its tremendous potential applications in packaging [5], agriculture [6], medical materials [7], Dong *et al* prepared the PLLA coating film through poly(ethylene glycol) as the media, the testing resultant showed the PLLA coating film had a good interfacial binding force and lower CO_2 and O_2 permeability. The effects of the PLLA coating film on sensory quality and microbial propagation in strawberries indicated that, when the PLLA coating film was used for strawberry, the PLLA coating film as an antimicrobial was effective [8].

However, for the native PLLA, slow crystallization speed is one of the worst negative properties and the resulting poor heat resistance has limited its wide practical application, because the molding process needs a long time and becomes a high-cost manufacturing process. Therefore, in an effort to improve crystallization ability of PLLA, a recent trend is to add a nucleating agent in PLLA matrix, thanks to its simple operation, low dosage, easy industrialization and efficient crystallization accelerating role [9-11].

**email: mci651@163.com*

The nucleating agent can instantaneously increase the nucleation density in PLLA matrix and reduce the surface free energy barrier to induce the crystallization to occur in the higher temperature region or at a faster cooling rate. As a result, the crystallization of PLLA has been improved by a large amount of effective nucleating agents such as talc [12], montmorillonite [13], mica [14], halloysite [15], calcium carbonate [16], zinc citrate [17], silicon dioxide [18], grapheme [19], YVO_4 [20], metal phosphonate [21], zinc salts of amino acids [22], metallic salts of phenylmalonic acid [23], *p*-tert-butylcalix[8]arene [24], myo-inositol [25], sorbitol derivative [26, 27], *fulvic acid amide [28], benzoyl hydrazine derivatives [29, 30], 1H-benzotriazole derivatives [31], etc.* Through analysis of progress in nucleating agents for PLLA, it was found that the nucleating agent for PLLA gradually evolved from inorganic compounds to organic compounds [32]. For the organic nucleating agents, the inherent disadvantage of poor compatibility of inorganic nucleating agents with PLLA matrix can be effectively avoided, and organic nucleating agents also present better nucleation effect for PLLA as compared to the inorganic nucleating agents [33]. Therefore, further developing efficient organic nucleating agents to finally realize large-scale application is very important to PLLA industry.

Unfortunately, compared to the nucleating agents for other thermoplastics like polypropylene and polyethylene, the category and quantity of organic nucleating agents for PLLA need to be still further expanded. Given that, in this work, the isophthalic dihydrazide and piperonylic acid derived from the pepper were used to synthesis *N, N′*-isophthalic bis(piperonylic acid) dihydrazide (PAID) as a new organic nucleating agent for PLLA. Then the PAID-nucleated PLLA was fabricated by melt blending technology, and the thermal performances including non-isothermal crystallization, melting behavior and thermal decomposition under flowing air, and mechanical properties of PLLA containing different PAID concentration were investigated in detail.

2.Materials and methods

PLLA in this work was obtained from Shenzhen Danshen Plastic Co., LTD, and the trade name of this PLLA was 4032D produced by Nature Works LLC of USA. All reagents used to synthesise PAID were obtained from Chongqing Huanwei Chemical Company of China, and these reagents were required to be analytical purity.

PAID synthesis

The synthetic route of PAID includes two steps, they are chlorination reaction and acylation reaction as shown in Figure 1. The typical synthesis procedure of PAID was as follows: the 10 g piperonylic acid together with the 70 mL thionyl chloride as solvent and 0.5 mL DMF as catalyst were mixed, and the mixture was slowly heated with stirring to reflux for 36 h. After the mixed solution was cooled to room temperature, the evaporation of the mixed solution in vacuum was performed, and the residue was piperonyloyl chloride.

The 0.004 mol isophthalic dihydrazide, 120 mL *N, N*-dimethylformamide and 3 mL triethylamine were mixed to form an homogeneous solution using ultrasonic technology, and then the 0.008 mol piperonyloyl chloride was added into the aforementioned mixed solution to be further stirred in an ice bath for 2 h, followed by heating up to 80ºC and hold for 6 h. The reaction mixture was poured onto 300 mL deionized water; after cooling, the suspension was filtrated, followed by further washing for three time using the deionized water. The resulting product was dried in vacuum at 35ºC. Fourier Transform Infrared Spectrometer (FT-IR) υ: 3383.8 cm^{-1} (N-H stretching vibrations absorption); 3084.9 and 746.9 cm^{-1} (C–H stretching vibration and the out-of-plane bending vibration absorption); 1685.3 cm^{-1} (stretching vibration absorption of C=O of synthesized amide group); 1647.9 (stretching vibration absorption of C=O of isophthalic dihydrazide); 1608.2, 1585.8, 1505.1 and 1446.5 cm^{-1} (vibration absorption of C–C of benzene); 1325.1 cm^{-1} (stretching vibration of C–N and bending vibration of N–H). ^{1}H Nuclear Magnetic Resonance (^{1}H NMR) δ: ppm; 10.04 (s, 1H, NH), 8.46 (s, 1H, NH), 7.00~7.51 (m, 3H, Ar), 6.11 (s, 2H, Ar). 2920.3,

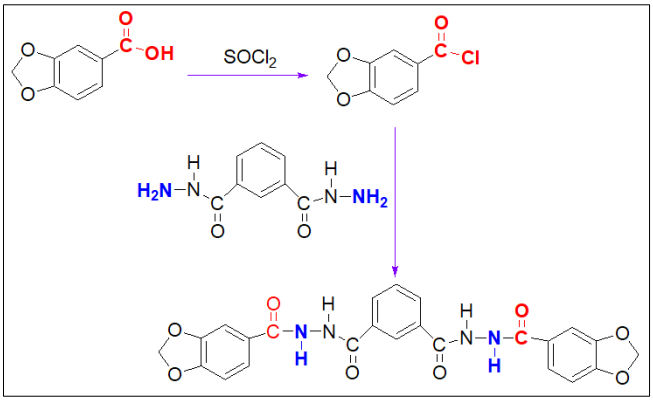

Figure 1. synthetic route of PAID

Preparation of PLLA/PAID samples

Before the blend, the PLLA and PAID need to be thoroughly dried for 48 h at 35ºC under vacuum to remove the residual water. The molten state blend of PLLA with different PAID concentration (0.5 wt%, 1 wt%, 2 wt% and 3 wt%) was carried out in on a counter-rotating mixer. The blending temperature was set to 190 ºC, and the screw speeds were set at 32 rpm for 7 min and 64 rpm for 7 min, respectively. In the presence of 20 MPa, the aforementioned mixture was further hot pressed at 180ºC and cool pressed at room temperature for 5 min to obtain the relevant samples with a thickness of 0.4 mm. Finally, the prepared PLLA samples containing 0.5 wt% PAID, 1 wt% PAID, 2 wt% PAID and 3 wt% PAID were named PLLA/0.5%PAID, PLLA/1%PAID, PLLA/2%PAID and PLLA/3%PAID, respectively.

Test and characterization

The FT-IR and ^{1}H NMR characterization of the PAID were recorded on an IS50 spectrometer and AVANCE 400MHz nuclear magnetic resonance instrument, and the FT-IR testing sample of PAID was prepared *via* the standard KBr pellet, and the spectra measurement was performed in a wavenumber range of 4000 to 400 cm^{-1}; the deuterium reagent for ^{1}H NMR measurement was dimethyl sulfoxide. The melt-crystallization and cold-crystallization measurements were conducted on a Q2000 DSC with 50 mL/min nitrogen. For the melt-crystallization process, the sample was heated to the set melting temperatures (170ºC, 180ºC, 190ºC and 200ºC) to maintain at that temperature for 3 min to eliminate heat history, and then the sample was cooled at different cooling rates (1ºC/min, 5ºC/min, 10ºC/min, 20ºC/min, 30ºC/min, 40ºC/min and 50ºC/min) to record the melt-crystallization DSC curve. For the cold-crystallization process, the sample was heated to the 190ºC to hold for 3 min, then the sample was quenched to 40ºC to hold for 3 min, and the sample was heated at different heating rates (1ºC/min, 2 ºC/min, 5ºC/min, 10ºC/min) to record the cold-crystallization DSC curve. The melting process of the sample was still recorded by DSC, after melt-crystallization at cooling rate of 1 ºC/min, the sample was heated at different heating rates (1 ºC/min, 2ºC/min, 5ºC/min, 10ºC/min) to record the melting process; and the sample was heated to 190ºC to hold for 3 min to be quenched to the set crystallization temperatures (120ºC, 125ºC, 130ºC, 135ºC and 140ºC), held at that temperature for 180 min to ensure complete crystallization, and then the sample was heated to 190ºC at a heating rate of 10ºC/min to record the melting DSC curve. The thermal decomposition behavior of the sample was determined by Q500 TGA with 60 mL/min flowing air, and the sample was heated from 35 to 650ºC at a heating rate of 5ºC/min. The mechanical properties testing of the sample with dimensions of 25 mm×4 mm×0.5 mm were operated on a D&G DX-10000 electronic tensile tester with 1 mm/min stretching speed.

3.Results and discussions

Melt-crystallization behavior

Upon cooling of 1 ºC/min, the DSC curves of the pure PLLA and PLLA/PAID were shown in Figure 2. For the pure PLLA, there is almost not melt-crystallization peak in DSC curve as reported by literature

[34, 35], attributed to the poor nucleation ability of PLLA itself. Usually, the total crystallization process includes two stages, the nucleation and crystal growth. The poor nucleation ability of PLLA itself results in the very slow nucleation rate and the formation of no nuclei. In contrast with the pure PLLA, all PLLA/PAID samples exhibit the obvious and sharp melt-crystallization exotherms in DSC curves, indicating that the PAID has the positive role of accelerating the crystallization of PLLA. This result is thought to be due to the heterogeneous nucleation of PAID for PLLA crystallization, because the PAID can provide a large amount of heterogeneous nuclei in PLLA matrix during cooling, and the existence of these heterogeneous nuclei leads to the fast nucleation rate; on the other hand, the initial high temperature region of cooling of the melt ensures the mobility of PLLA molecular chain and the fast crystal growth rate; as a result, the melt-crystallization peak appears in the DSC curves. Figure 2 also displays the influence of PAID concentration on the crystallization process of PLLA, it is found that, with increasing of PAID concentration, the melt-crystallization peak shifts toward higher temperature, and two important index parameters, namely the onset melt-crystallization temperature (T_{oc}) and the melt-crystallization peak temperature (T_{mc}), increase from 136.8°C and 132.2°C to 139.4°C and 135.2 °C, respectively. This result implies that a higher PAID loading can promote the crystallization to occur in a higher temperature region. In this study, 3 wt% PAID exhibits the better nucleation effect for PLLA's crystallization than other PAID concentration. Additionally, the temperature gap between T_{oc} and T_{mc} can effectively reflect the crystallization rate of semi-crystalline polymers; generally, the smaller the temperature gap is, the faster the crystallization rate is. Through the analysis of the temperature gap of PLLA/PAID sample, it is clear that the temperature gap decreases from 4.6°C to 4.2°C with increasing of PAID concentration from 0.5 wt% to 3 wt%, showing that a larger amount of PAID causes the PLLA to possess a faster crystallization rate. As far as the melt-crystallization enthalpy is concerned, the PLLA/1%PAID sample exhibits the largest melt-crystallization enthalpy of 49.3 J/g comparing with the 45.0 J/g for PLLA/0.5%PAID, 48.8 J/g for PLLA/2%PAID and 48.9 J/g for PLLA/3%PAID. However, according to the relevant crystallinity calculation equation [36], the ccrystallinity of PLLA/0.5%PAID, PLLA/1%PAID, PLLA/2%PAID, PLLA/3%PAID are 48.6%, 53.5%, 53.5% and 54.2%, respectively.

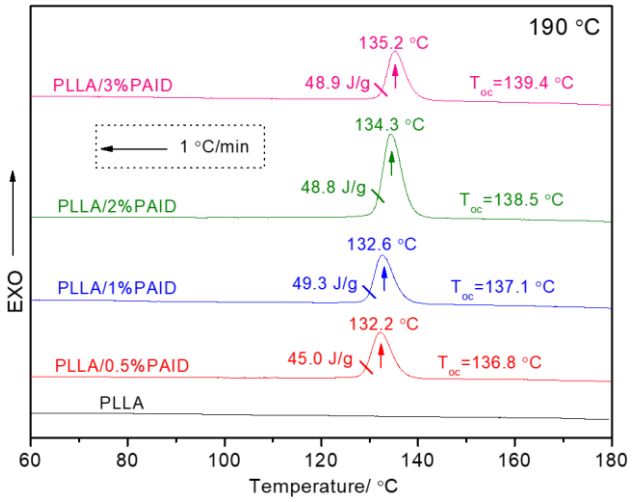

Figure 2. Melt-crystallization DSC curves of the pure PLLA and PLLA/PAID at a cooling rate of 1°C/min

For the practical injection molding, the crystallization is often expected to occur at a faster cooling rate. Thus, investigating on the melt-crystallization behavior of PLLA/PAID at a faster cooling rate is very constructive to practical production, which can also further demonstrate the nucleation ability of PAID for PLLA crystallization. Figure 3 shows the melt-crystallization DSC curves of PLLA/PAID samples from the melt of 190°C at different cooling rates. For a given PLLA/PAID sample, it is a fact that, with increasing of cooling rate, a wider melt-crystallization peak located at a lower temperature appears in DSC curve, the reason may be that at low cooling rate there is more time to overcome the nucleation barrier, in contrast, at high cooling rate nuclei become active at lower temperatures [37].

However, the crystallization of PLLA/2%PAID and PLLA/3%PAID samples is still able to be accelerated upon the fast cooling at 50ºC/min, identifying the advanced nucleation ability of PAID for PLLA's crystallization again. This result may be instrumental to the practical manufacturing.

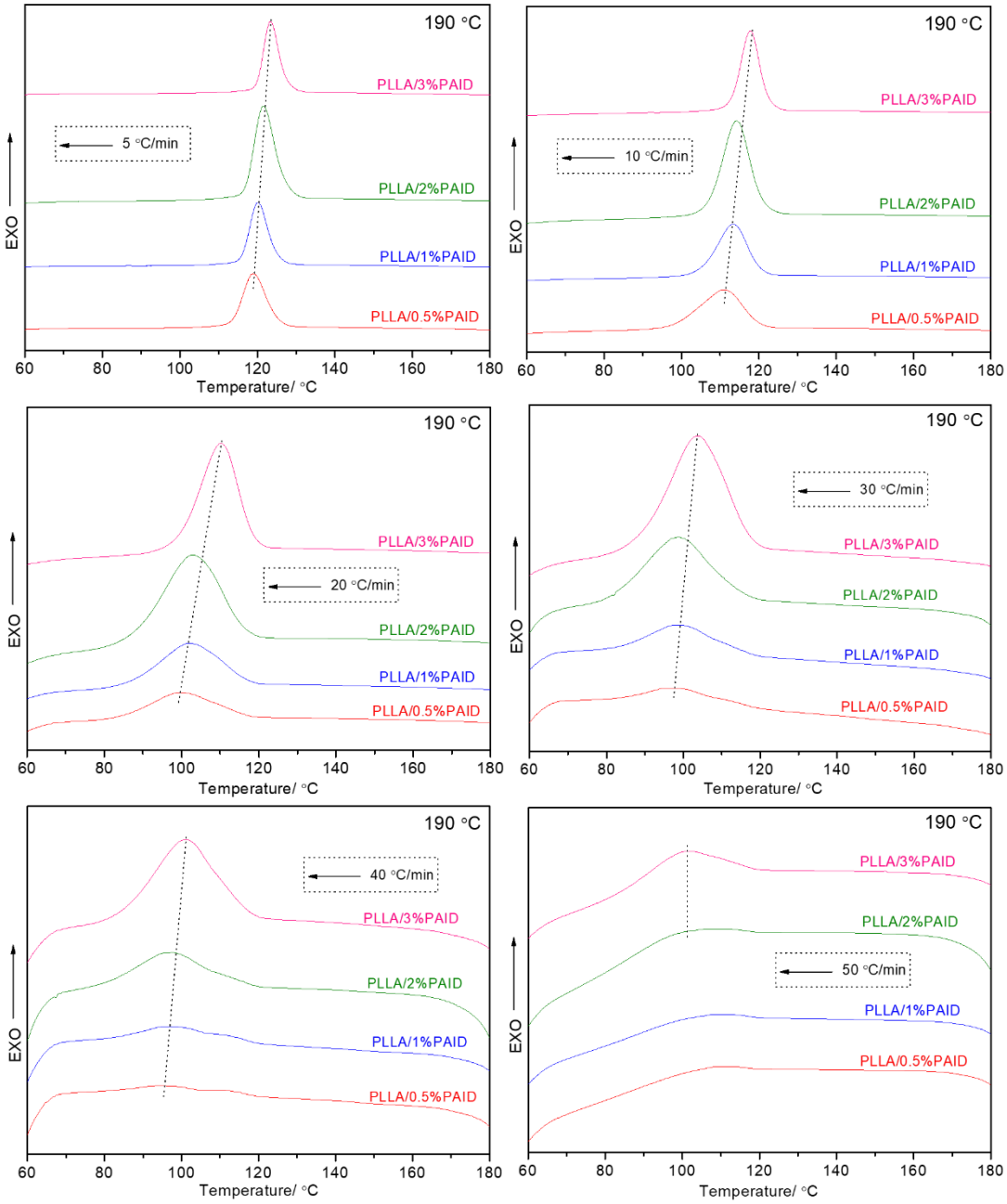

Figure 3. Melt-crystallization DSC curves of PLLA/PAID samples at different cooling rates

Besides the cooling rate, the influence of the set final melt temperature (T_f) on the crystallization process of PLLA is also further investigated by DSC. Figure 4 gives the melt-crystallization DSC curves of PLLA/PAID samples from the 180 or 200ºC at a cooling rate of 1ºC/min. Whether the T_f is 180 or 200ºC, the T_{oc}, T_{mc} and melt-crystallization enthalpy of a given PLLA/PAID sample are larger comparing with the relevant data obtained from the melt-crystallization from T_f of 190ºC. In particular, when the T_f is 200ºC, the melt-crystallization peak appears in the highest temperature region in DSC curve, indicating that the T_f of 200 ºC is highly favourable for the crystallization process of PLLA/PAID sample, because the solubility of organic nucleating agent in PLLA is strongly influenced by the T_f [34], and the higher T_f can cause more PAID to be dissolved in PLLA matrix, resulting in a better compatibility of

PAID with PLLA, as well as in better intermolecular interaction. This interaction of PLLA with PAID is a critical factor to promote the crystallization, becasuet the interaction can promote the PLLA molecular chain to attach to PAID surface. But a decrease of undissolved PAID must lead to a drop in nuclei, and the ultimate crystallization depends on the undissolved PAID and the interaction of PLLA with PAID. Under this circumstance, compared to a decrease of nuclei, the interaction presents a more important role in the promoting crystallization of PLLA.

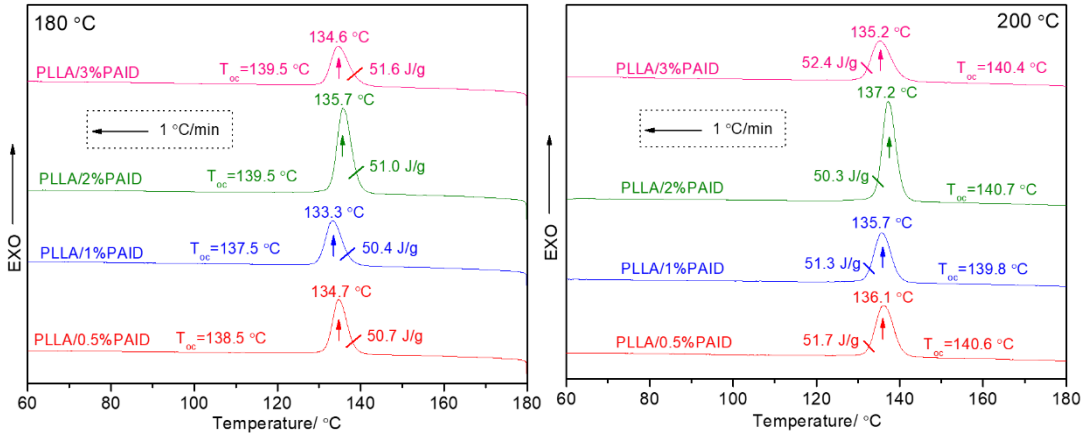

Figure 4. Melt-crystallization DSC curves of PLLA/PAID samples from the T_f at a cooling rate of 1 °C/min

However, when the T_f is 170 °C, the undissolved PAID exhibits a greater effect on the crystallization process of PLLA (Figure 5), because a melt-crystallization peak with a higher temperature location and height appears in DSC curve. That is, the T_{oc} and T_{mc} increase about 5～10 °C, respectively, even the T_{oc} is very close to 150 °C, which is about 5°C higher than the theoretical upper temperature of crystallization (the theoretical upper temperature is often 0.85 time of the melting temperature, and the melting temperature is about 165～170°C in this study, see the melting behavior section). Moreover, the temperature gap between T_{oc} and T_{mc} becomes smaller, even the temperature gap of the PLLA/3%PAID sample is only 0.4°C, showing a very fast crystallization rate. Additionally, the melt-crystallization enthalpy is up to 56.8 J/g, the crystallinity is 63.0%.

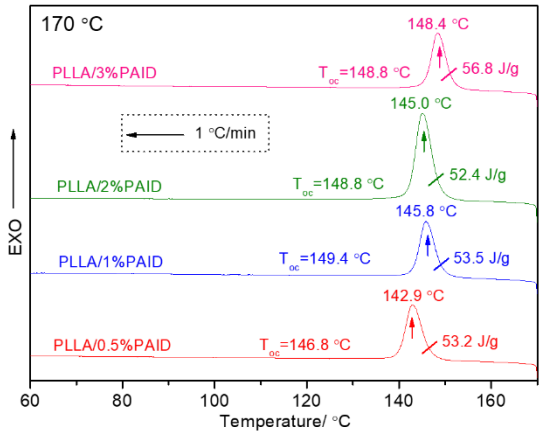

Figure 5. Melt-crystallization DSC curves of PLLA/PAID samples from the T_f of 170 °C at a cooling rate of 1 °C/min

In the above section, it is hypothesized that there exists an intermolecular interaction between PLLA and PAID. In order to confirm this hypothesis and propose probable nucleation mechanism of PAID for PLLA crystallization, a preliminary theoretical analysis was performed *via* DMol3 calculation of MS

software, and the optimized geometry structure and frontier orbital energy of the PAID and PLLA with repeating units were obtained (Figure 6). The detailed HOMO and LUMO of PAID are -0.2011 eV and -0.099 eV; the HOMO and LUMO are -11.082 eV and 0.251 eV for PLLA. According to the frontier orbital theory, the LUMO-HOMO energy gap between LUMO of PAID and HOMO of PLLA is 10.983 eV, which is smaller than 11.333 eV of LUMO-HOMO energy gap of PLLA itself, showing that the PLLA and PAID interact more easy at intermolecular level during the melting blend process. Through the further analysis of PLLA and PAID molecular structure, it is thought to be that the interaction probably appears at the C=O of PLLA and N-H of PAID, and this chemical interaction may be expected to be the nucleation mechanism of PAID for PLLA. This conclusion has to be confirmed by further work.

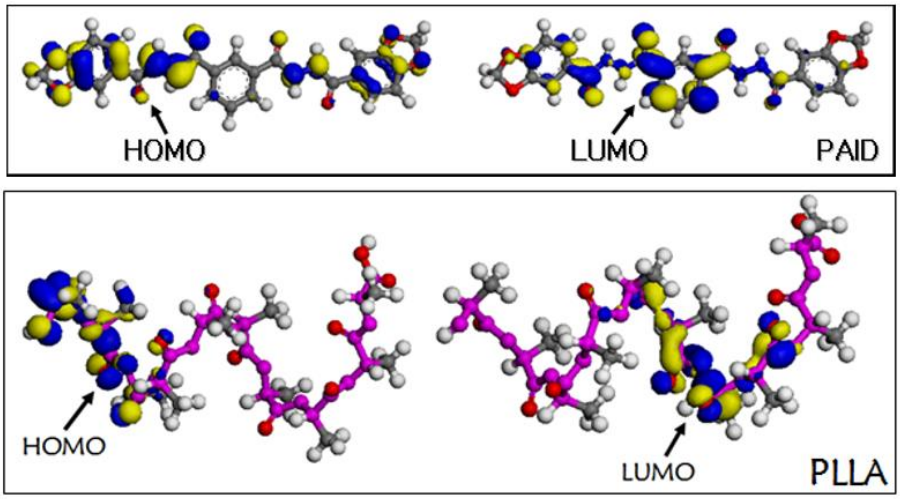

Figure 6. Frontier orbital energy of PAID and PLLA

Cold-crystallization behavior

Figure 7 gives the cold-crystallization processes of PLLA/PAID samples from 40°C at different heating rates. When the heating rate is 1°C/min, an increase of PAID concentration has an inhibition effect on the cold crystallization process of PLLA, because the cold-crystallization peak shifts toward the lower temperature. For cold-crystallization process, a large amount of nuclei from PLLA self-homogeneous nucleation and PAID heterogeneous nucleation supply the very fast nucleation rate. In this case, the crystal growth is the rate-determining step. Unfortunately, a larger amount of PAID often exhibit a higher negative effect on the mobility of PLLA molecular chain as reported [38], resulting in that it takes more time to complete the crystallization, and the formed peaks are flatter. According to the aforementioned process, the formed crystals relatively become more prefect because of a longer crystallization time, and this speculation is proved by the subsequent melting process. That is to say, the melting temperature appears at higher temperature with increasing of PAID concentration, because the higher melting temperature often means the more prefect crystals, and this effect only depends on the PAID concentration. In addition, as seen in Figure 7, for a given PLLA/PAID sample, an increase of heating rate leads to a shift toward the high temperature, the reason is thought to be the thermal inertia.

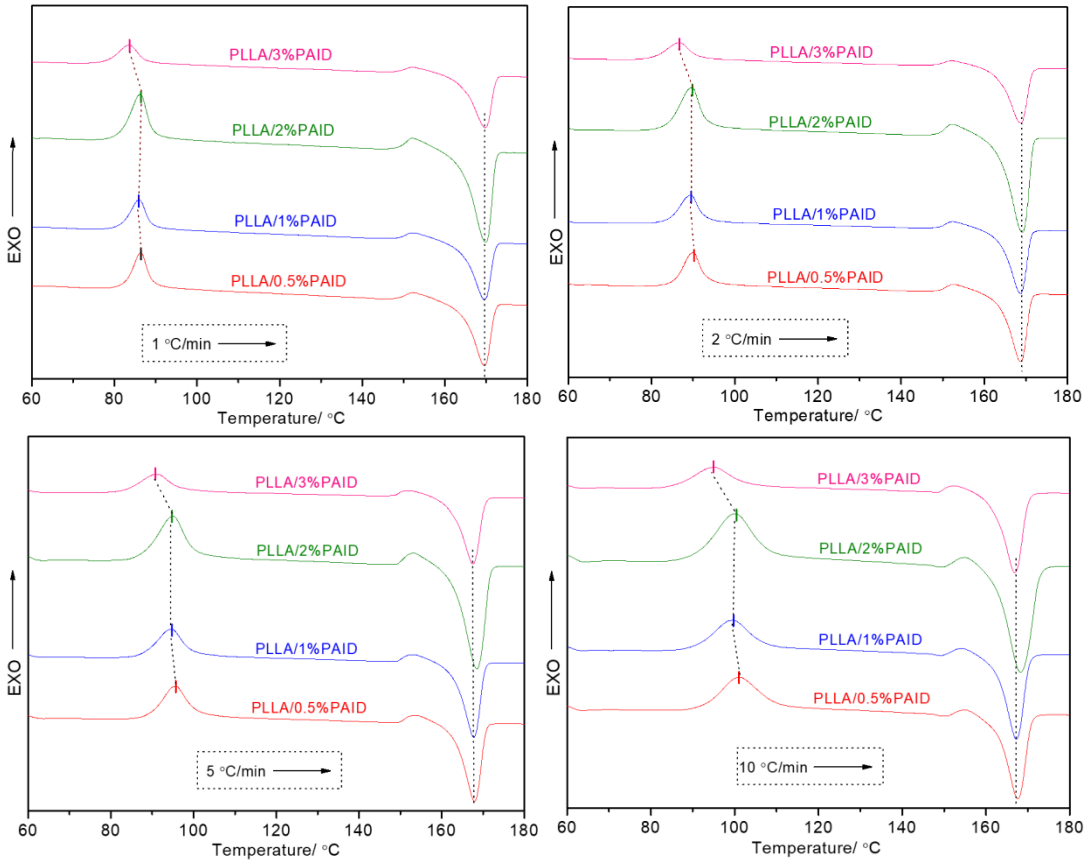

Figure 7. Cold-crystallization DSC curves of PLLA/PAID samples at different heating rates

Melting behavior

As aforementioned, the addition of PAID significantly changes the crystallization behavior of PLLA. Undoubtedly, the melting process of PLLA was also affected by the PAID, because the melting behavior of semi-crystalline polymer is closely related to the crystallization. Figure 8 gives the melting processes of all PLLA/PAID samples at a heating rate of 2°C/min and 10°C/min after the melt-crystallization upon cooling of 1 °C/min. It is clear that there exists only single melting peak in all DSC curves, indicating that the crystallization has almost been completed in cooling, and there are almost no new crystals formed during heating. With increasing of the heating rate, the melting peaks become wider, which is still attributed to the thermal inertia. In other words, an increase of the heating rate gives no enough time for the crystals to melt at set temperature, and so the melting only occurs at higher temperature.

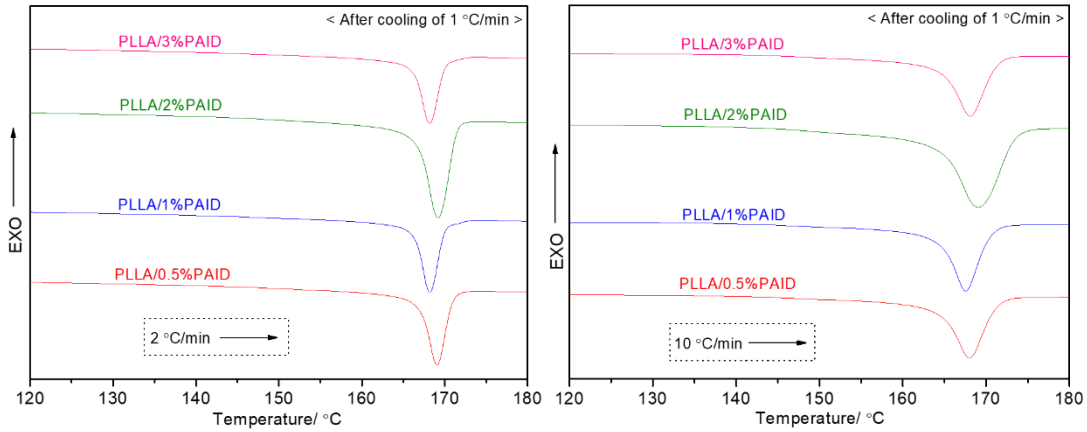

Figure 8. Melting processes of PLLA/PAID samples at different heating rates after melt-crystallization

In theory the crystallization of semi-crystalline polymer can occur in the temperature region from the glass transition temperature to the melting temperature. Selecting the suitable temperature, which can ensure the optimum growth rate in presence of PAID, is very important to rapidly complete crystallization. Thus, the melting processes of PLLA/PAID samples after the adequate isothermal crystallization at different crystallization temperatures was studied (Figure 9). As shown in Figure 9, DSC curve only exhibit the single melting peak. On the hand, the undissolved PAID and enough time make the crystallization be completed; on the other hand, the excellent molecular chain mobility in heating causes the crystal growth to become more difficulty. Thus, the single melting peak appears in DSC curve. Additionally, with increasing of crystallization temperature, the melting peak of a given PLLA/PAID sample moves toward the higher temperature, the probable reason is that the PLLA molecular chain has the better mobility in the higher temperature, and the crystals can be fully grown to obtain the relatively perfect crystal, especially in the case of full crystallization. As a result, the corresponding melting peak appears at higher temperature. However, an increase of crystallization temperature also makes the melting peak become wider, meaning the widening of melting range. The high mobility of PLLA molecular chain is instrumental in crystal growth, but the high mobility also may lead to the larger difference in crystal size.

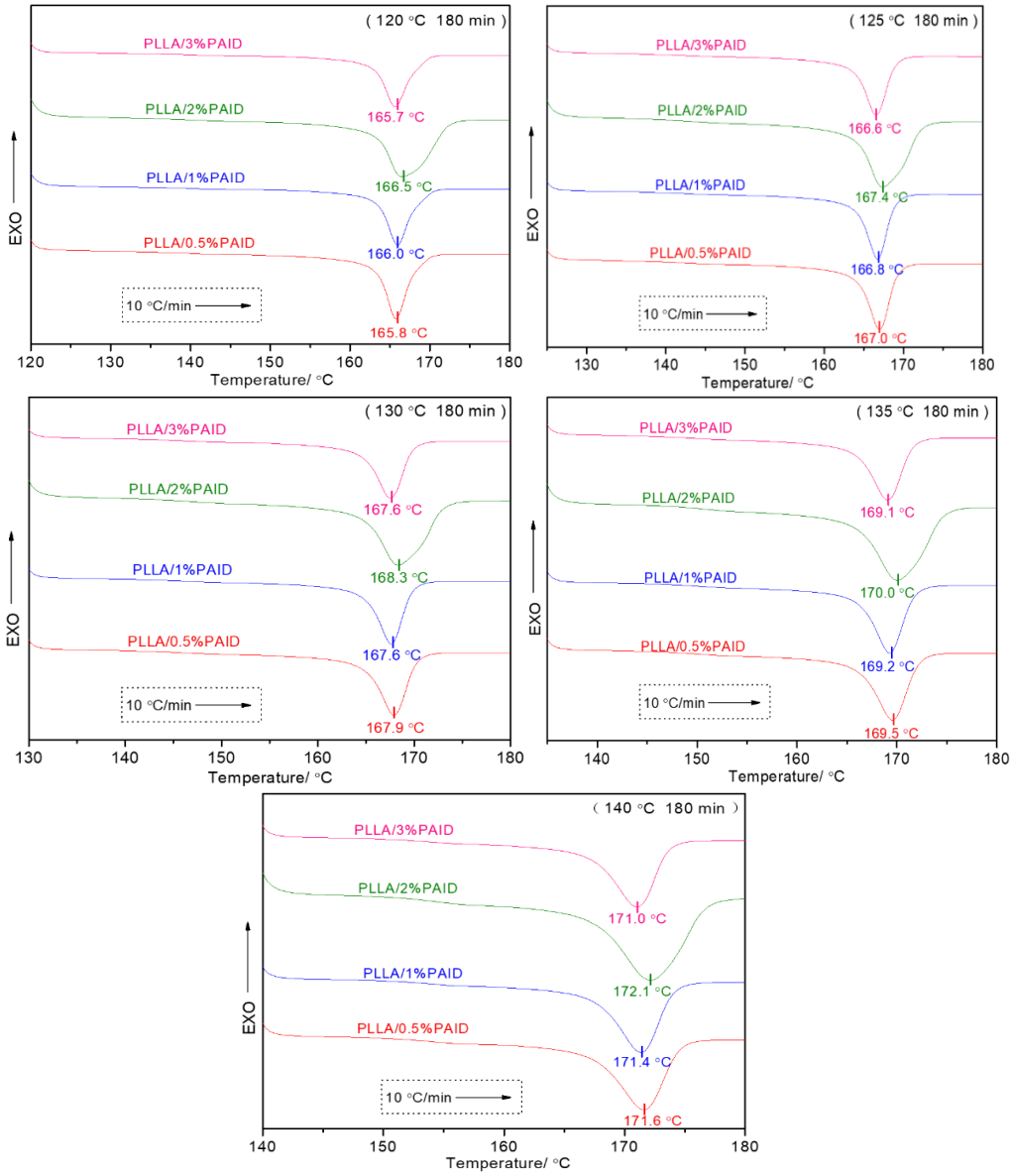

Figure 9. Melting processes of PLLA/PAID samples after isothermal crystallization at different temperatures for 180 min

Thermal stability

If the introduction of PAID seriously decreased the thermal decomposition temperature under air, the PAID-nucleated PLLA products do not have usefulness. Figure 10 shows the TGA curves of PLLA/PAID samples from 40 to 650ºC at a heating rate of 5 ºC/min. All PLLA/PAID samples similar to the pure PLLA have only one thermal decomposition stage in TGA curves, meaning that the thermal decomposition profile of PLLA is not dramatically changed. Two probable reasons are used to explain this result: the excellent compatibility of PAID with PLLA and the low dosage of PAID. However, the presence of PAID in PLLA resin slightly decreases the onset thermal decomposition temperature (T_{od}), and the T_{od} at 341.3ºC, 335.1ºC, 334.9ºC, 336.0ºC and 335.0ºC is relevant to the pure PLLA, PLLA/0.5%PAID, PLLA/1%PAID, PLLA/2%PAID and PLLA/3%PAID, respectively. Compared to the T_{od} of the pure PLLA, the minimum T_{od} of PLLA/PAID is 334.9 ºC, and the maximum difference is only 6.4ºC, which can meet the application requirement in terms of thermal stability. However, among the PLLA/PAID samples, the T_{od} exhibits irregular trend with increasing of PAID concentration, moreover, the difference in T_{od} is very tiny. This effect depends on the two factors of the PAID concentration and intermolecular interaction, the introduction of PAID with low T_{od} decreases the T_{od} of PLLA/PAID sample, but the existence of this intermolecular interaction can prevent the decrease of T_{od}, because this intermolecular interaction is firstly destroyed in heating [39, 40].

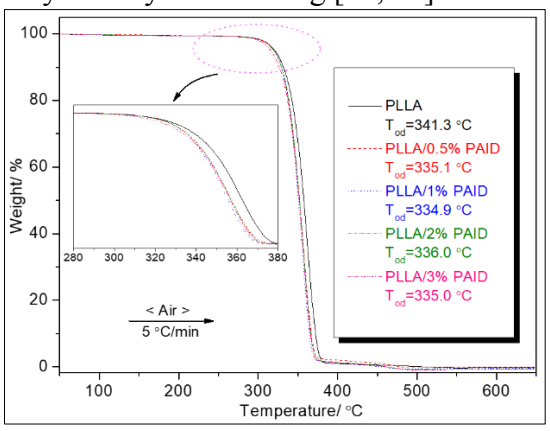

Figure 10. TGA curves of PLLA/PAID samples

Mechanical properties

A comparison on the mechanical properties of the pure PLLA and PLLA/PAID samples is shown in Figure 11. With the addition of PAID, the elongation at break continuously decreases from 6.9 to 3.9%, this effect may depend on the rigidity of organic small molecule PAID itself and the crystallization promoting role of PAID for PLLA, because an increase of the rigidity and crystallinity can cause the PLLA to become more brittle. For the tensile strength, although the tensile strength exhibits a downward trend with a higher loading level of PAID in PLLA matrix, all PLLA/PAID samples have a larger tensile strength than the pure PLLA, and the PLLA/0.5%PAID sample has the maximum tensile strength value of 60.9 MPa, which is about 1.5 times with respect to the pure PLLA.

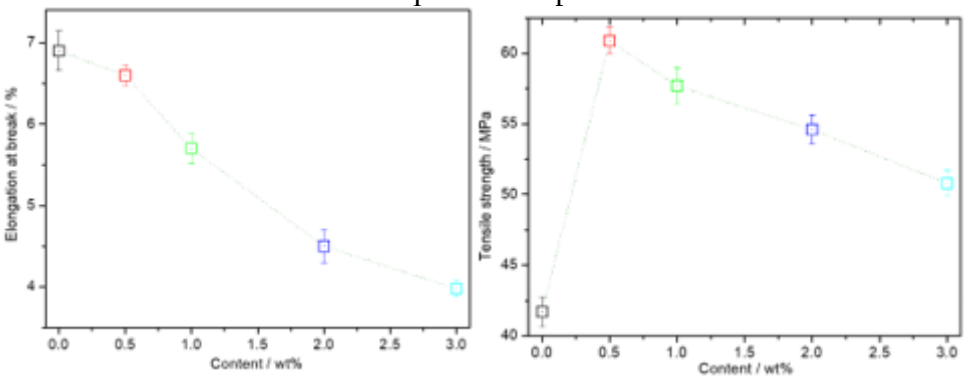

Figure 11. The elongation at break and tensile strength of the pure PLLA and PLLA/PAID sample

4.Conclusions

In this work, the crystallization accelerating effect of PAID for PLLA was confirmed *via* the melt-crystallization process, and when the T_f was 190ºC, the 3 wt% PAID had the best nucleation promoting ability for PLLA, even the T_{oc} is almost close to the 140ºC upon the cooling of 1ºC/min. Although an increase of cooling rate weakened the crystallization promoting ability of PAID, the PLLA/PAID sample could still accelerate the crystallization speed of PLLA upon fast cooling at 50 ºC/min. Additionally, the T_f exhibited a complicated effect on the melt-crystallization of PLLA, because this effect depended on the compatibility of PLLA with PAID and undissolved PAID; and the PLLA/PAID sample had the best crystallization ability when the T_f was 170ºC. The frontier orbital energy calculations of PLLA and PAID implied that the nucleation mechanism of PAID for PLLA was attributed to the intermolecular interaction. However, the addition of PAID exhibited the negative effect on the cold-crystallization behavior of PLLA because of PAID's hindrance of the mobility of PLLA molecular chain. The difference in melting behavior of PLLA/PAID samples could adequately reflect the heating conditions and the previous crystallization derived from the melt-crystallization process and isothermal crystallization. Compared to the pure PLLA, the presence of PAID in PLLA resin only led to a slight decrease in T_{od}, and maybe this result can further confirmed the existence of the intermolecular interaction between PLLA and PAID. As well as the PLLA/PAID sample had the higher tensile strength, but the PLLA containing a larger amount of PAID exhibited a consecutive decrease in the elongation at break.

Additionally, more in-depth works, including the effect of PAID on the size of the crystals, nucleation mechanism and the minimum amount of undissolved PAID in PLLA matrix, need to be conducted in a future study to thoroughly reveal the role of PAID.

Acknowledgements. This work was supported by National Natural Science Foundation of China (project number 51403027), Foundation of Chongqing Municipal Science and Technology Commission (cstc2017shmsA20021 and cstc2019jcyj-msxmX0876), Scientific and Technological Research Program of Chongqing Municipal Education Commission (project number KJQN201801319), and Foundation of Yongchuan District (project number Ycstc, 2018cc0801).

References

1. GENG ZX, ZHEN WJ, SONG ZB, WANG XF. Structure and performance of poly(lactic acid)/amide ethylenediamine tetraacetic acid disodium salt intercalation layered double hydroxides nanocomposites [J], Journal of Polymer Research, 2018, 25: 115
2. TACHIBANA Y, MAEDA T, ITO O, MAEDA Y, KUNIOKA M. Biobased myo-inositol as nucleator and stabilizer for poly(lactic acid) [J], Polymer Degradation and Stability, 2010, 95(8): 1321-132
3.HAN LL, PAN PJ, SHAN GR, BAO YZ. Stereocomplex crystallization of high-molecular-weight poly(L-lactic acid)/poly(D-lactic acid) racemic blends promoted by a selective nucleator [J], Polymer, 2015, 63: 144-153
4. XIE Q, CHANG XH, QIAN Q, PAN PJ, LI CY. Structure and Morphology of Poly(lactic acid) Stereocomplex Nanofiber Shish Kebabs [J], ACS Macro Letters, 2020, 9(1): 103-107
5. RHIM JW, PARK HM, HA CS. Bio-nanocomposites for food packaging applications [J], Progress in Polymer Science, 2013, 38: 1629-1652
6. KYRIKOU I, BRIASSOULIS D. Biodegradation of agricultural plastic films: a critical review [J], Journal of Polymers and The Environment, 2007, 15: 125-150
7. ZHOU ZH, RUAN JM, ZHOU ZC, ZOU JP, CHEN LL. Preparation and properties of bioactive composite based on bioactive glass and Poly-L-lactide [J], Polymer-Plastics Technology and Engineering, 2008, 47: 451-457
8. YUN XY, LI XF, DONG T. Preparation and characterization of poly(L-lactic acid) coating film for strawberry packaging [J], Science of Advanced Materials, 2019, 11(10): 1488-1499

9. XU XK, ZHEN WJ, BIAN SZ. Structure, performance and crystallization behavior of poly(lactic acid)/humic acid amide composites [J], Polymer-Plastics Technology and Engineering, 2018, 57(18): 1858-1872
10. CAI YH, ZHAO LS, ZHANG YH. Role of *N, N′*-bis(1H-benzotriazole) adipic acid acethydrazide in crystallization nucleating effect and melting behavior of poly(L-lactic acid) [J], Journal of Polymer Research, 2015, 22: 246
11. SI PF, LUO FL, XUE P, YAN DG. Crystallization mechanism, microstructure and mechamical property of poly(L-lactic acid) modified by introduction of hydrogen bonding [J], Journal of Polymer Research, 2016, 23: 118
12. PETCHWATTANA N, NARUPAI B. Synergistic effect of talc and titanium dioxide on poly(lactic acid) crystallization: An investigation on the injection molding cycle time reduction [J], Journal of Polymers and the Environment, 2019, 27(4): 837-846
13. WU T, TONG YR, QIU F, YUAN D, ZHANG GZ, QU JP. Morphology, rheology property, and crystallization behavior of PLLA/OMMT nanocomposites prepared by an innovative eccentric rotor extruder [J], Polymers for Advanced Technologies, 2018, 29(1): 41-51
14. SOUZA DHS, ANDRADE CT, DIAS ML. Isothermal crystallization kinetics of poly(lactic acid)/synthetic mica nanocomposites [J], Journal of Applied Polymer Science, 2014, 131(11): 40322
15. KAYGUSUZ I, KAYNAK C. Influences of halloysite nanotubes on crystallization behavior of polylactide [J], Plastics Rubber and Composites, 2015, 44(2): 41-49
16. LIANG JZ, ZHOU L, TANG CY, TSUI CP. Crystalline properties of poly(L-lactic acid) composites filled with nanometer calcium carbonate [J], Composites Part B-Engineering, 2013, 45(1): 1646-1650
17. TERANISHI S, KUSUMI R, KIMURA F, KIMURA T, ABURAYA K, MAEYAMA M. Biaxial Magnetic orientation of zinc citrate as nucleating agent of poly(L-lactic acid) [J], Chemistry Letters, 2017, 46(6): 830-832
18. HAKIM RH, CAILLOUX J, SANTANA OO, BOU J, SANCHEZ-SOTO M, ODENT J, RAQUEZ JM, DUBOIS P, CARRASCO F, MASPOCH ML. PLA/SiO_2 composites: Influence of the filler modifications on the morphology, crystallization behavior, and mechanical properties [J], Journal of Applied Polymer Science, 2017, 134(10): 45367.1-45367.12
19. AJALA O, WERTHER C, NIKAEEN P, SINGH RP, DEPAN D. Influence of grapheme nanoscrolls on the crystallization behavior and nano-mechanical properties of polylactic acid [J], Polymers for Advanced Technologies, 2019, 30(7): 1825-1835
20. EI-TAWEEL SH, ABBOUDI M. Nonisothermal crystallization kinetics of PLA/nanosized YVO_4 composites as a novel nucleating agent [J], Journal of Applied Polymer Science, 2020, 137(5): 48340
21. PAN PP, LIANG ZC, CAO A, INOUE Y. Layered metal phosphonate reinforced poly(L-lactide) composites with a highly enhanced crystallization rate [J], ACS Applied Materials & Interfaces, 2009, 1(2): 402-411
22. WEI ZY, SHAO SN, SUI ML, SONG P, HE MM, XU Q, LENG XF, WANG YS, LI Y. Development of zinc salts of amino acids as a new class of biocompatible nucleating agents for poly(L-lactide) [J], European Polymer Journal, 2019, 118: 337-346
23. LI CL, DOU Q. Effect of metallic salts of phenylmalonic acid on the crystallization of Poly(L-lactide) [J], Journal of Macromolecular Science, Part B: Physics, 2016, 55(2): 128-137
24. SHI YQ, WEN L, XING Z. Study on the crystallization activation energy of poly(L-lactic acid) nucleated with *p*-tert-butylcalix[8]arene [J], Polymers & Polymer Composites, 2018, 26(2): 169-175
25. SHI H, CHEN X, CHEN WK, PANG SJ, PAN LS, XU N, LI T. Crystallization behavior, heat resistance, and mechanical performances of PLLA/myo-inositol blends [J], Journal of Applied Polymer Science, 2017, 134(16): 44732
26. PETCHWATTANA N, NAKNAEN P, SANETUNTIKUL J, NARUPAI B. Crystallization behavior and transparency of poly(lactic acid) nucleated with dimethylbenzylidene sorbitol [J], Plastics Rubber and Composites, 2018, 47(4): 147-155

27. SUN C, LI CX, TAN HY, ZHANG YH. Enhancing the durability of poly(lactic acid) composites by nucleated modification [J], Polymer International, 2019, 68(8): 1450-1459
28. LIU PY, ZHEN WJ. Structure-property relationship, rheological behavior, and thermal degradability of poly(lactic acid)/fulvic acid amide composites [J], Polymers For Advanced Technology, 2018, 29(8): 2192-2203
29. FAN YQ, YAN SF, YIN JB. The relationship between solubility and nucleating effect of organic nucleating agent in poly(L-lactic acid) [J], Journal of Applied Polymer Science, 2019, 136(7): 46851
30. CAI YH, YAN SF, YIN JB, FAN YQ, CHEN XS. Crystallization behavior of biodegradable poly(L-lactic acid) filled with a powerful nucleating agent-N, N'-bis(benzoyl) suberic acid dihydrazide [J], Journal of Applied Polymer Science, 2011, 121(3): 1408-1416
31. CAI YH, TANG Y, ZHAO LS. Poly(L-lactic acid) with organic nucleating agent N, N, N'-tris(1H-benzotriazole) trimesinic acid acethydrazide: Crystallization and melting behavior [J], Journal of Applied Polymer Science, 2015, 132(32): 42402
32. LIU PY, ZHEN WJ. Structure-property relationship, rheological behavior, and thermal degradability of poly(lactic acid)/fulvic acid amide composites [J], Polymers for Advanced Technologies, 2018, 29: 2192-2203
33. SONG P, SANG L, ZHENG LC, WANG C, LIU KK, WEI ZY. Insight into the role of bound water of a nucleating agent in polymer nucleation: a comparative study of anhydrous and monohydrated orotic acid on crystallization of poly(L-lactic acid) [J], RSC Advances, 2017, 7(44): 27150-27161
34. FAN YQ, ZHU J, YAN SF, CHEN XS, YIN JB. Nucleating effect and crystal morphology controlling based on binary phase behavior between organic nucleating agent and poly(L-lactic acid) [J], Polymer, 2015, 67: 63-71
35. ZHAO LS, CAI YH, LIU HL. *Physical properties of poly(L-lactic acid) fabricated using salicylic hydrazide derivative with tetraamide structure [J], Polymer-Plastics Technology and Materials, 2020, 59(2): 117-129*
36. KAWAMOTO N, SAKAI A, HORIKOSHI T, URUSHIHARA T, TOBITA E. Nucleating agent for poly(L-lactic acid) - An optimization of chemical structure of hydrazide compound for advanced nucleation ability [J], Journal of Applied Polymer Science, 2007, 103(1): 198-203
37. DI LORENZO ML, RUBINO P, COCCA M. Isothermal and non-isothermal crystallization of poly(L-lactic acid)/poly(butylene terephthalate) blends [J], Journal of Applied Polymer Science, 2014, 131(12): 40372
38. JOZIC SP, JOZIC D, ERCEG M, ANDRICIC B, BERNSTORFF S. Nonisothermal crystallization of poly(L-lactide) in poly(L-lactide)/olive stone flour composites [J], Thermochimica Acta, 2020, 683: 178440
39. LIAO YZ, XIE MH, LI MC. Hydrogen-bonding interactions and miscibility in *N, N*-dilauryl chitosan/poly(l-lactide) blend membranes by solution approach [J], Chemical Industry and Engineering Progress, 2007, 26(5):725-730 (In Chinese)
40. CAI YH, ZHAO LS. Investigating on the modification of *N, N′*-adipic bis(benzoic acid) dihydrazide on poly(L-lactic acid) [J], Polymer Bulletin, 2019, 76(5): 2295-2310

Manuscript received: 21.03.2020